Chemometrics and Intelligent Laboratory Systems 167 (2017) 113–122

Contents lists available at ScienceDirect

Chemometrics and Intelligent Laboratory Systems

journal homepage: www.elsevier.com/locate/chemometrics

Principal Component Analysis to interpret changes in chromatic parameters on paint dosimeters exposed long-term to urban air

Agustín Herrera [a], Davide Ballabio [b], Natalia Navas [c], Roberto Todeschini [b], Carolina Cardell [a, *]

[a] Dept. of Mineralogy and Petrology, Faculty of Science, University of Granada, Campus Fuentenueva s/n, 18071 Granada, Spain
[b] Dept. of Earth and Environmental Sciences, University of Milano-Bicocca, P.za della Scienza 1, 20126 Milano, Italy
[c] Dept. Analytical Chemistry, and Biomedical Research Institute of Granada (IBIG), University of Granada, Faculty of Science, Campus Fuentenueva s/n, E 18071 Granada, Spain

ARTICLE INFO

Keywords:
Chromatic parameters
Principal Component Analysis
Portable spectrophotometer
Proteinaceous paint dosimeters
Urban atmosphere

ABSTRACT

Atmospheric pollutants can originate the decay of historic paintings exposed to the outdoor elements. This is a cause of great concern, since such contaminants can produce physical-chemical alterations manifested initially in undesirable color change. This paper tests an unsupervised multivariate approach on discrete data color parameters in a pioneering study which combines spectrophotometric data and principal components analysis to detect unaesthetic color change on paint dosimeters in (semi)open-air monuments exposed long-term to the urban atmosphere of the city of Granada (South Spain). To this end the chromatic parameter of the CIEL*a*b* and CIEL*C*h* systems (L*, a*, b*, h*, C* and ΔE) were used as variables for subsequent multivariate analysis in order to determine the intrinsic color change trends. The aim is to evaluate the specific chromatic parameter(s) that cause the unaesthetic damage for each type of paint dosimeter, while also considering the influence of the binder (egg yolk/rabbit glue), the pigment (azurite, malachite and lapis lazuli) and for the first time, the grain size of the studied pigments (azurite). Results demonstrated that this approach is capable of discriminating samples on the basis of dosimeter composition, so enabling interpretation of their aging process. Azurite and lapis lazuli-laden dosimeters tended to turn green over time as a result of exposure to city air regardless of binder composition and location. By contrast, all malachite-laden dosimeters became bluer over time. Luminosity remained stronger in dosimeters prepared with collagen, an important parameter in binder discrimination. This information is also of great value for restoration purposes.

1. Introduction

Over the last two decades cultural heritage conservation (e.g. historic buildings, wall paintings, sculptures, mosaics, archaeological sites, etc.) has focused on preventive conservation policies and procedures to reduce the need for more complex and costly restoration work [1]. To accomplish this, a range of conservation activities have been carried out inside buildings such as museums, churches and art galleries, and even in caves and catacombs, to prevent damage to artworks. This work normally includes assessment of the environmental conditions, typically temperature (T), relative humidity (RH), light and UV levels, as well as the effects of pollutants, microorganisms and visitors [2–4], and their impact on the artworks [5–7]. Given that a large amount of indoor artworks are paintings or have polychrome decoration, model samples (paint dosimeters or mock-ups) made with artists' materials (pigments and binders) that replicate the composition of the paint used by the original artists have been used to evaluate the damage they suffer, due to the effects of different indoor environments [8–10]. Since color change is the most evident effect of the impact of these environmental parameters on paint, chromatic measurements are commonly performed to assess the degree of aesthetic damage over time [11–13].

Although most works of art are stored indoors in museums and galleries, some important paintings, for example on the façades of historical buildings, are directly exposed to the outdoor city air. The atmospheric pollutants it contains can cause physical-chemical alterations in the paint that are manifested in undesirable color change. Nonetheless few studies have addressed the impact of polluted atmospheres on artworks of this kind [6,14–17]. Similarly, very little research has been done on paint dosimeters exposed long-term to urban polluted air, so as to monitor color changes that manifest underlying changes in the mineralogical composition of the pigments, binder oxidation and the precipitation of new crystalline phases or dust deposition [17–19].

* Corresponding author.
E-mail address: cardell@ugr.es (C. Cardell).

http://dx.doi.org/10.1016/j.chemolab.2017.05.007
Received 17 February 2017; Received in revised form 7 April 2017; Accepted 6 May 2017
Available online 19 May 2017

In the last decades, in the field of Cultural Heritage, statistical multivariate analyses such as Principal Component Analysis (PCA) have been applied to spectral data produced by diverse analytical techniques conducted on samples from real artworks or from reproductions made in the laboratory, such as e.g. Raman micro-spectroscopy (RMS), Fourier transform infrared spectroscopy (FTIR), Gas chromatography–mass spectrometry (GC-MS), Matrix-Assisted Laser Desorption Ionization Time of Flight Mass Spectrometry (MALDI-TOF-MS), Fiber optics reflectance spectroscopy (FORS). These multivariate analyses can handle large data bases and extrapolate the most meaningful information from the data. PCA has proved to be a useful tool for fast data representation and interpretation [13,20], identification of pigments and binders [21–24], assessing their state of conservation and distinguishing between natural and synthetic pigments [25]. However papers combining chemometric techniques with reflectance spectra obtained from spectrophotometers in the visible region (400–700 nm) are still rare in any field of science [26,27]. To the authors' knowledge this is the first paper to use PCA to analyze color changes in paint dosimeters exposed to the outdoor elements.

This paper presents a pioneering study which combines spectrophotometric data (in situ portable spectrophotometer) and PCA to detect undesirable color changes on paint dosimeters exposed long-term to the urban atmosphere in the city of Granada (South Spain). To this end the chromatic parameters of the CIEL*a*b* and CIEL*C*h* systems (L*, a*, b*, h*, C* and ΔE) were used as variables for subsequent multivariate analysis. The aim is to identify the specific chromatic parameter(s) that cause the unaesthetic damage for each type of paint dosimeter, while also considering the influence of the binder (egg yolk/rabbit glue) and, for the first time, the grain size of the studied pigments (azurite, malachite and lapis lazuli).

The final goal is to provide useful information that can be used to draw up preventive conservation strategies to safeguard these artworks. This problem is worse in hot cities with heavy traffic near the Mediterranean coast, such as Granada [4,6,28,29], famous for the Alhambra Palace, which contains a number of (semi)outdoor paintings. Granada's old quarter also has historical buildings with outdoor wall paintings, as does its Albayzín district, a UNESCO world heritage site.

2. Materials and methods

2.1. Painting materials

We selected two proteinaceous binders and three historical pigments to prepare the paint dosimeters. They were chosen after being identified in paint used in diverse artworks in (semi)open-air monuments in the city of Granada [30,31]. The painting materials were purchased from Kremer Pigments GmbH & Co. KG (Madrid, Spain). The natural pigments were malachite ($Cu_2CO_3(OH)_2$), lapis lazuli ($Na_{8\text{-}10}Al_6Si_6O_{24}S_{2\text{-}4}$) and azurite ($Cu_3(CO_3)_2(OH)_2$), whose references and grain sizes (according to the manufacturer) are: malachite natural standard with ϕ < 120 μm (ref: K10300), lapis lazuli ϕ < 80 μm (ref: K10540), and azurite with five different grain sizes which include various “azurite MP” and the “azurite natural standard”; these are: azurite MP extra deep (ref: K10203, ϕ = 80–100 μm), azurite MP deep (ref: K10204, ϕ = 80-63 μm), azurite MP pale (ref: K10206, ϕ = 63-38 μm), azurite MP sky-blue (ref:K10207, ϕ = <38 μm), and azurite natural standard deep greenish blue (ref: 10200, ϕ = <120 μm). MP refers to Michel Price, who in 1997 established a method for the separation of powdered azurite into different grades, representing different hues of blue [32]. This method was adopted by Kremer Pigments GmbH & Co. KG in 1998 to prepare a new variety of azurite pigments called “azurite MP.”

The chosen proteinaceous binders were rabbit glue (fine grind pearls from Kremer Pigments GmbH & Co. KG, ref. 63028) and natural egg yolk (from eggs purchased at the local market). Both binders were widely used during the Middle Ages and the Renaissance, and have been found in outdoor paintings in the city of Granada [31]. The names for the paint dosimeters were formed by adding the letters G (for glue) and E (for egg yolk) to the pigment labels (see Table 1), so as to clearly differentiate the powder pigments from the binary (pigment/binder) paint mixtures.

2.2. Paint dosimeters

Fourteen paint dosimeters were prepared according to old master recipes to mimic the real egg yolk-based or rabbit glue-based tempera used by medieval artists. In the tempera painting technique, pigments are finely ground and mixed with water, then solidified by blending with a proteinaceous binder. Seven paint dosimeters were composed of a pure pigment blended with the egg yolk binder, while the other seven dosimeters were blended with the rabbit glue binder [33]. The procedure to prepare the egg yolk binder can be found in Herrera et al. [17] and that for the rabbit glue binder in Cardell et al. [19]. To obtain the pure binder dosimeters each fluid paste was spread directly onto a glass slide.

The tempera paint dosimeters were prepared as follows: circa 0.5 g of each pigment powder was placed in a small bowl and several drops of the binder (each pigment requires different amounts) were added to form a fluid paste. Then, to prepare the binary paint dosimeter, several fine layers of the pastes were spread onto a glass slide with a paintbrush, so as to emulate the real paint layers found in ancient paintings.

2.3. Natural air pollution aging test

The paint dosimeters were naturally aged by exposing them to the urban atmosphere of the city of Granada (South Spain). To this end, sets of dosimeters were placed in selected (semi)open-air monuments with varying air quality (Fig. 1). Some of the monuments are situated in the city center (~650 m above sea level), and thus are more affected by heavy traffic; these are the Cathedral, the *Corral del Carbón*, the Hospital of *San Juan de Dios*, and the Church of *Santo Domingo*. The rest of the dosimeters were positioned in monuments on the city's two hills, the Albayzín and al-Sabika. The dosimeters in the Albayzin were placed in the *Palacio del Almirante* (~100 m above the city center), while three sets of dosimeters were installed in the *Alhambra and Generalife* monumental complex (on the al-Sabika hill, ~200 m above the city center), as follows: one set in the Harem (Alhambra) and two sets in the Generalife in two rooms at slightly different altitudes (Fig. 1). These dosimeters were exposed to the urban air for 18 months. In situ non-invasive color measurements were performed with a portable spectrophotometer after 1, 2, 3, 4, 6, 10 weeks, 6 months, 12 months and 18 months. During the exposure period the paint dosimeters were subjected to the effects of major construction works, heavy traffic, sunlight irradiation, rain, cold, heat and wind.

Table 1
Features of the analyzed blue pigments.

Kremer pigment reference	Kremer pigment size	Grain size according to [19]	Authors pigments reference	Paint dosimeter reference (authors)
Malachite natural standard Nº 10300	<120 μm	2.5 μm very extra fine	MAL-VEF	MAL-VEF-E MAL-VEF-G
Azurite MP extra deep Nº 10203	100-80 μm	90 μm extra coarse	AZ-EC	AZ-EC-E AZ-EC-G
Azurite MP deep Nº 10204	80-63 μm	70 μm coarse	AZ-C	AZ-C-E AZ-C-G
Azurite MP pale Nº 10206	63-38 μm	45 μm medium	AZ-M	AZ-M-E AZ-M-G
Azurite MP sky-blue Nº 10207	<38 μm	25 μm extra fine	AZ-EF	AZ-EF-E AZ-EF-G
Azurite natural standard Nº 10200	<120 μm	<22 μm very extra fine	AZ-VEF	AZ-VEF-E AZ-VEF-G
Lapis lazuli Nº 10540	<80 μm	47 μm medium	LAP-M	LAP-M-E LAP-M-G

Note: VEF = very extra fine; EC = extra coarse; C = coarse; M = medium; EF = extra fine; E = Egg Yolk; G = Rabbit Glue.

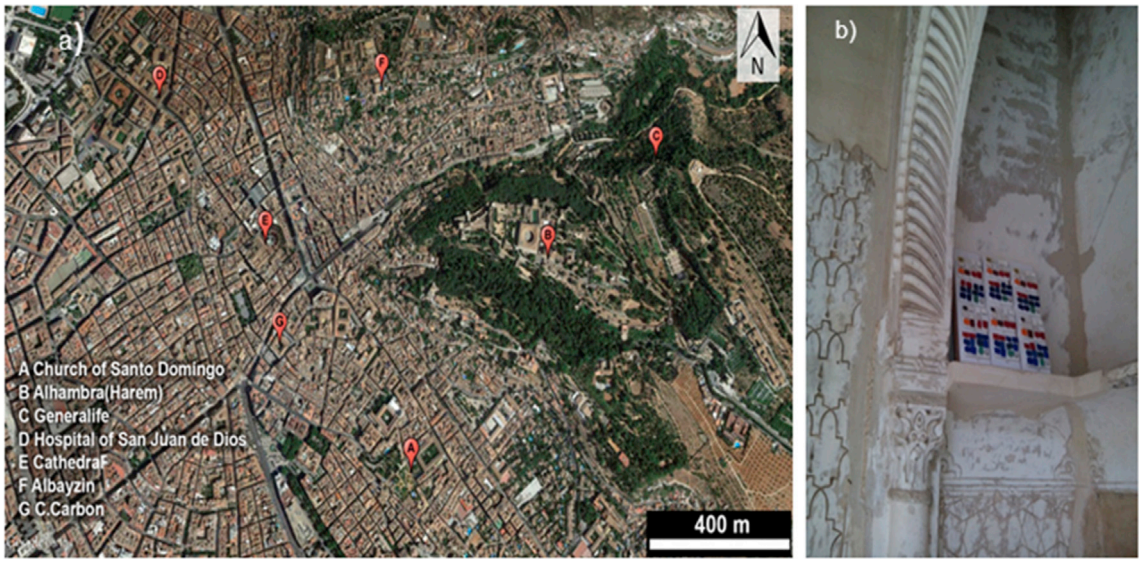

Fig. 1. (a) Aerial view of the city of Granada (South Spain) showing the location of the paint dosimeters at (semi)open monuments; (b) set of paint dosimeters placed in the *Harem* of the Alhambra monument.

2.4. Color measurements

The chromatic characteristics of the paint dosimeters were studied with a Minolta CM-700d portable spectrophotometer using an 8 mm measuring aperture. The standard daylight illuminant D65 (color temperature: 6504 K) was applied. Results are presented in alphanumeric color codes of the CIEL*a*b* and CIEL*C*h* systems. In the CIEL*a*b* system, L* represents luminosity, varying from black (0) to white (100); a* ranges from −a* (green) to +a* (red), and b* from −b* (blue) to +b* (yellow).

In the CIEL*C*h* color system each color is represented by means of three angular parameters or cylindrical coordinates, most closely related to the psychophysical perception of the color: L*, lightness or luminosity of color, also defined in both scalar and angular color sets; chroma or saturation ($C^* = (a^{*2}+b^{*2})^{1/2}$) related to the intensity of color and the hue angle (h* = arctan (b*/a*)) or tone of color, which refers to the dominant wavelength and indicates redness, yellowness, greenness or blueness on a circular scale, starting at 0° and increasing counterclockwise, i.e. 0° is "red", 90° is "yellow", 180° is "green" and 270° is "blue" [34]. CIEL*a*b* color difference (ΔE) is the Euclidean distance between two points in the color space [34]. This distance is typically expressed as ΔE, where: ($\Delta E = (\Delta L^*)^2+(\Delta a^*)^2+(\Delta b^*)^2)^{1/2}$. Note that when ΔE has three units or more, it is considered to be a color change that can be perceived by the human eye.

2.5. Principal Component Analysis (PCA)

Data were arranged in a numerical matrix with samples on the rows and variables (L*, a*, b*, H*, C* and ΔE) on the columns. In order to detect data patterns and clusters, the data structure was analyzed using PCA, which is a well-known multivariate pattern recognition technique [35]. PCA was calculated on auto-scaled data (mean-centering and unit variance scaling) since variables had different scales and units, such that auto-scaling was needed in order to standardize them and make them comparable for the subsequent multivariate analysis [13,36]. Principal Component Analysis was performed by means of the PCA toolbox for MATLAB [35] and SpectraMagic X (spectrophotometer) for the data obtained from color measurements.

3. Results and discussion

PCA is a well-known chemometric technique for unsupervised data analysis by projecting data in a reduced space, defined by orthogonal principal components, i.e. PCs [37]. With this in mind, we used all the samples analyzed in the entire study to look for similarities and differences beyond the obvious color characteristics, i.e. green for malachite-laden dosimeters and blue for lapis lazuli and azurite-laden dosimeters. To this end, PCA was performed on a data matrix comprising 1086 measured of colors (rows), each described by the 6 variables (columns) related with the intrinsic color parameters, i.e. L*, a*, b*, H*, C* and ΔE.

In previous studies, PCA has been applied on continuous color data, i.e. using reflectance spectra [38]. In this paper, we propose an innovative way to track color changes based on the use of discrete data, i.e. the chromatic parameters L* (luminosity), a* (red/green), b* (yellow/blue), H* (tone of color), C* (chroma or saturation) and ΔE (total color difference), which are used in the CIEL*a*b* and CIEL*C*h* systems. The information obtained by applying PCA to these color parameters enables easier visualization and interpretation of the color change trends occurring in all the dosimeters.

Table 1 supplemental file shows the statistical parameters of the PCA performed on this entire data set. PC1 had a high explained variability value of 62%, and similarly high values were obtained for PC2 (19%) and PC3 (16%). PC4 and PC5 only accounted for 1% and 0.6% of total explained variability respectively. We therefore decided to base the interpretation of the data on the first three PCs (98% of the variability included in the original data set).

The information encoded in these three PCs is shown in Fig. 2. The loading plot of PC1 *vs* PC2 (Fig. 2a) indicated that L* and b* (yellow/blue hues) have the highest positive weight on PC1, while the color tone (H*) and a* (red/green hues) have the highest negative values. The two remaining variables i.e. C* and ΔE, have little influence on this PC1 and have higher weight on PC2. Fig. 2b (loading plot of PC1 *vs* PC3) shows that ΔE has the highest weight on PC3, followed by L* and C*.

Fig. 3a displays changes in the color parameters of all the paint dosimeters (at the various selected monuments), which shows the score of the dosimeters on the first three PCs. Each point on the score plot represents a dosimeter, which means that relationships and similarities between the dosimeters can be deduced from the clusters. For a better comprehension of the Figures, hereafter the scores have been colored differently based on the specific factors being studied in this paper, i.e. pigment composition, pigment particle size, type of binder mixed with the pigment, and exposure time to urban air. In Fig. 3, sample scores were colored on the basis of the pigment composition of the paint dosimeter. Fig. 3a shows that the paint dosimeters were clearly grouped together

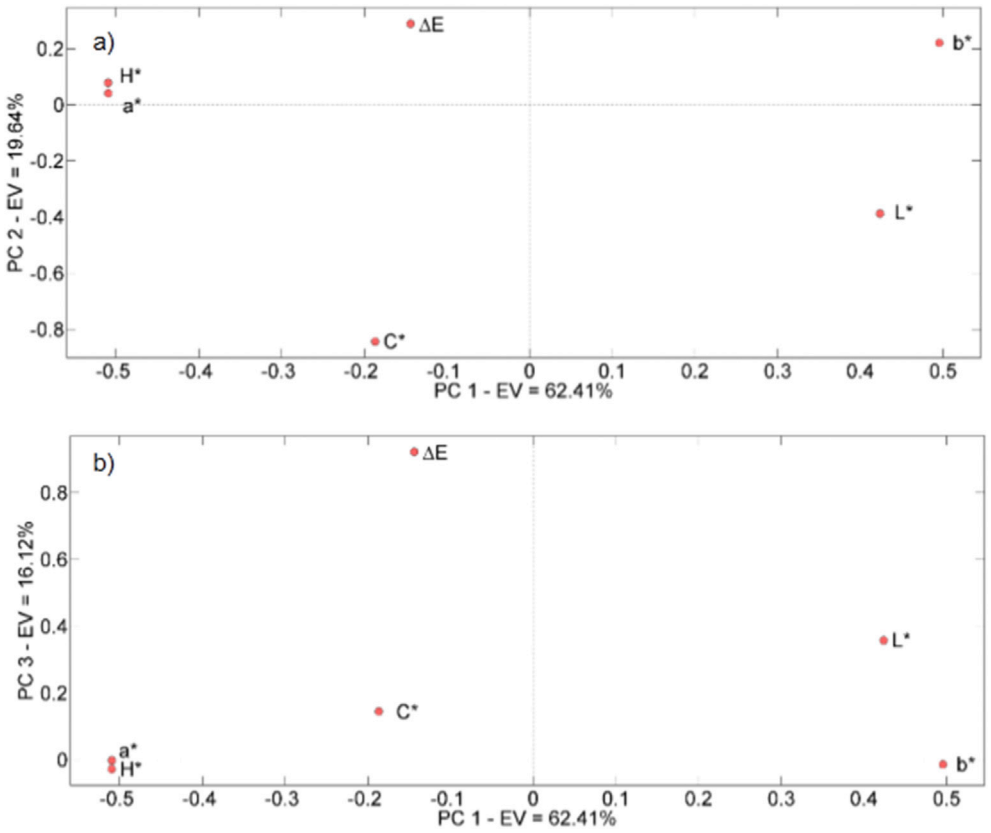

Fig. 2. Loading plot of the PCA performed using all the paint dosimeters: (a) loading plot of PC1 *vs* PC2; (b) loading plot of PC1 *vs* PC3.

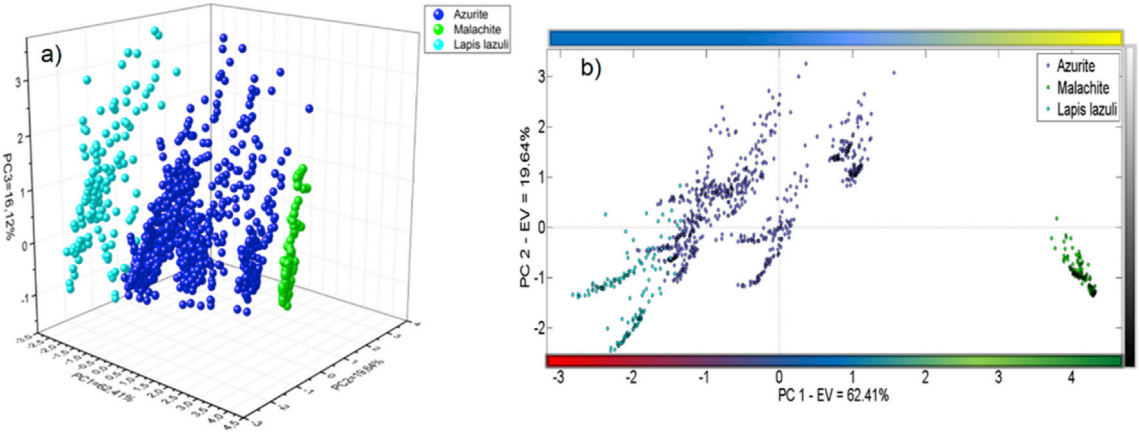

Fig. 3. PCA results for all the paint dosimeters (each pigment colored differently): (a) score plot PC1 *vs* PC2 *vs* PC3; (b) score plot PC1 *vs* PC2.

according to their respective colors using the information contained in the three first PCs, which accounted for 98% of the explained variability. This initial inspection indicates that the color of the pigment in the dosimeter is the key factor enabling us to discriminate between the dosimeters, rather than exposure time to urban air or the type of binder used in the paint. Hence, as shown in Fig. 3a, all malachite-laden dosimeters (green) were clearly clustered at the highest values on PC1 (at positive values), far away from the other samples (blue).

As Fig. 3a reveals, azurite and lapis lazuli-based dosimeters were well clustered and were close to each other. In these samples a clear tendency was observed in the analysis of the PC1 and PC2 as shown in Fig. 3b. The score for the lapis lazuli-laden dosimeters increased with exposure time to urban air such that after 18 months it had reach similar values to those of the azurite-laden dosimeters at the beginning of the experiment. The scores for azurite-laden dosimeters on PC1 and PC2 also increased with exposure time to air pollution.

Fig. 3b also clearly shows that in the blue dosimeters (made of either lapis lazuli or azurite) there is a noticeable effect that distributes them in PC1 and PC2 in the same direction with increasing exposure time to urban air. Thus, parameters such as H^*, C^*, ΔE and the tendency to yellow hues ($+b^*$) and green hues ($-a^*$) increase with exposure to urban air. As regards discrimination among the three types of pigments, although the three PCs are related with a total discrimination based on the pigment used in the paint dosimeter, they can be partially grouped by using the score samples on PC1. This indicates that color parameters such as a* (red/green), b* (yellow/blue), H* and L* have greater weight than ΔE and C* to discriminate these dosimeters based on the pigment composition (see Fig. 2a).

We performed a more detailed analysis of the results using two-dimensional score plots of the first three PCs as shown in Fig. 4a–d. In each Figure the scores were colored differently according to the particular variable that could influence color change in the paint dosimeters. These variables were: i) the type of binder - the scores were colored either blue (rabbit glue) or red (egg yolk) (Fig. 4a and b); ii) the time exposed to urban air - the different exposure times were given different colors (Fig. 4c); and iii) the pigment grain size - the scores for the different crystal sizes of the pigments were colored differently.

As regards the type of binder, a close inspection of the clusters was carried out in order to ascertain whether the binders could produce a sufficient degree of discrimination to enable us to group the dosimeters according to exposure time to urban air. Fig. 4a shows that PC1 and PC2 could discriminate the type of binder (egg yolk or rabbit glue) in certain paint dosimeters. The AZ-VEF (i.e. azurite standard according to Kremer manufacturer, see Table 1) dosimeters were clustered according to binder composition, i.e. egg yolk or rabbit glue. Indeed, those with egg yolk content had slightly lower scores on PC1 than the samples with rabbit glue binder. This means that AZ-VEF-E dosimeters tend to become more yellow and green than AZ-VEF-G dosimeters (Fig. 4a). However, as shown in Fig. 4b, when the scores are represented on PC1 and PC3, only malachite-laden samples are grouped according to the type of binder. Hence MAL-VEF dosimeters have the highest b* and L* values and a* exhibit the most negative values as expected for the green malachite color (Fig. 2b). The MAL-VEF-G dosimeters are the greenest and brightest of all the samples studied.

PCA results assessing the aging of the samples at different times over the 18 months experimental period are shown in Fig. 4c. In this case the combination of PC1 and PC3 was also checked and it proved to be even more informative than PC1 vs PC2, as it allowed us to discern a relationship with exposure over time. Results showed that at the beginning of the outdoor aging test LAP-M dosimeters scored high values on PC1 (red hues, i.e. a* values and tone, H*) and low values on PC3 (total color differences, ΔE) (see Fig. 2b for loading interpretation). At the beginning of the aging test these dosimeters were bluer but over time tended to become greener. The malachite-laden samples by contrast had high scores at the beginning of the test for the yellow parameter (+b*) and L*, and very low green hues (-a*), tone (H*) and color differences (ΔE), which resulted in a more yellowish color and higher luminosity than the other pigments. These dosimeters, which display the lowest total color variations (ΔE), are also the least damaged. In addition, in azurite-laden dosimeters the a*, b*, H* and L* loading values on PC1 and PC2 are neither very positive or very negative. Instead, these dosimeters have the highest C* and ΔE values on PC3. This means that the azurite-laden dosimeters experienced the highest changes in saturation and total color of all the paints we studied.

The effect of the pigment grain size on variation of color parameters is shown in Fig. 4d. Five different grain sizes were checked to evaluate whether there is any relationship between pigment particle size and the tendency to age in the urban air of Granada. If we examine the score plots in Fig. 4d, it is clear that the AZ-EF and AZ-VEF samples are separated in PC1, irrespective of the binder used, as AZ-VEF samples have scores greater than 0, while AZ-EF samples have scores lower than 0. If we look at the loading plots (see Fig. 2a), the AZ-VEF dosimeters tend to be the greenest (highest -a* values) of all the azurite-laden dosimeters. AZ-VEF and AZ-EF also show the highest total color variation of all the paint samples we studied.

When the sample scores were colored according to the sites of the dosimeters in different open-air monuments in Granada (see Fig. 1 supplemental file), PCA was unable to extract any information regarding the impact of the different air quality scenarios, in that sample score distribution was not related with the location of the dosimeters. This indicates that the location of the paint dosimeters is less important in producing color changes than the type of pigment present in the paint, at least over

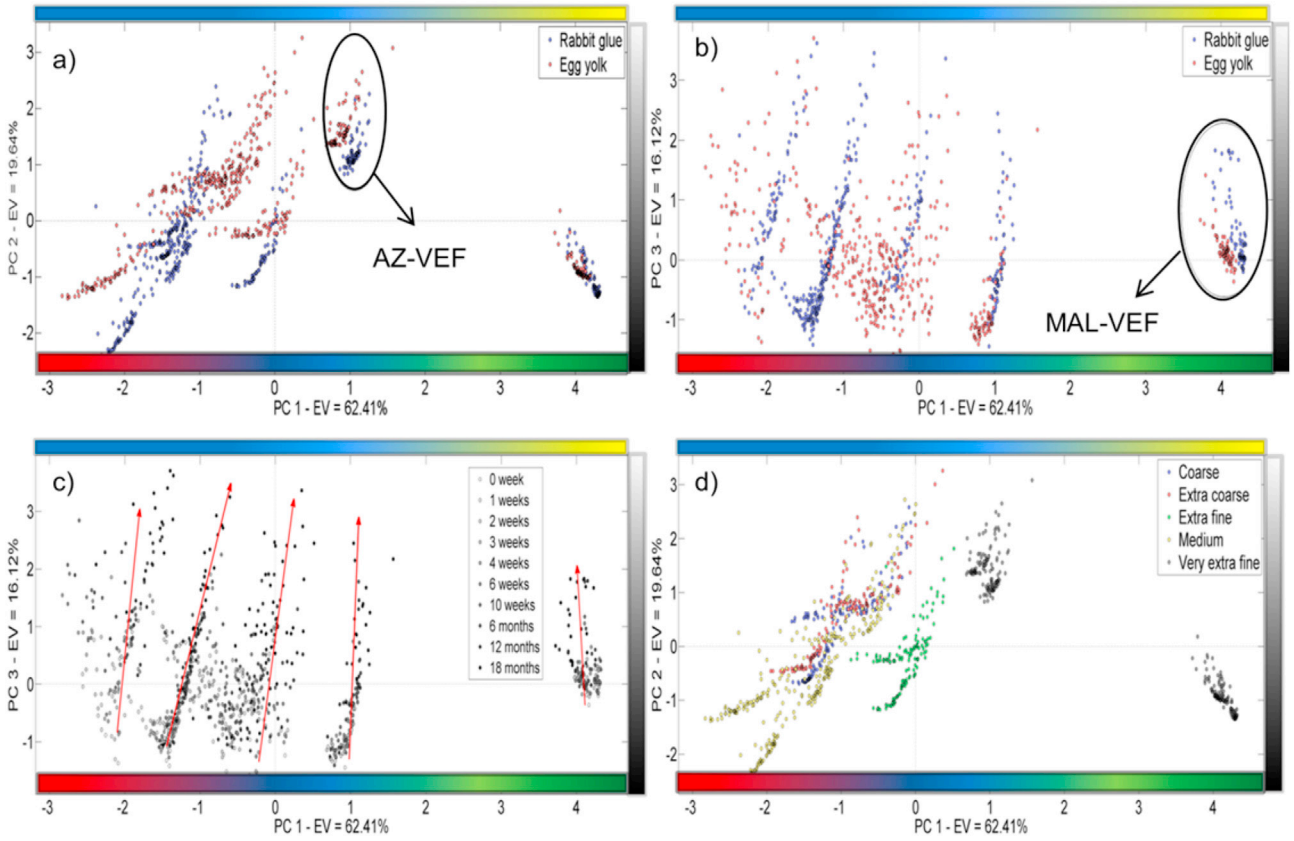

Fig. 4. Score plots for all paint dosimeters: (a) samples colored by binder represented in PC1 and PC2; (b) samples colored by binder represented in PC1 and PC3; (c) samples colored by exposure time represented in PC1 and PC3; (d) samples colored by grain size represented in PC1 and PC2. AZ = azurite; MAL = malachite; VEF = very extra fine grain size.

the period of the natural aging test, and for the pigments we studied. One exceptional, major visible color change was noticed after six months in the dosimeters AZ-EC-G, AZ-M-G and AZ-EF-G situated in the Generalife (see Fig. 1, label C), the highest point in the Alhambra monument complex and surrounded by gardens. This color change turned out to be unrelated with the aging process, and was caused by a discontinuous layer of pollen on the surface of the dosimeters that was visible with the naked eye.

A similar approach was used to extract information on each set of paint dosimeters containing the same pigment, i.e. malachite, lapis lazuli and azurite based dosimeters. Results are discussed below by pigment.

3.1. Malachite

When performing PCA on malachite-laden samples, we used a data matrix defined by 158 rows (malachite-laden dosimeters) and 6 columns (color parameters as variables). PCA indicated that the first two PCs explained 90% of total data variance (Table 2 supplemental file). Fig. 5

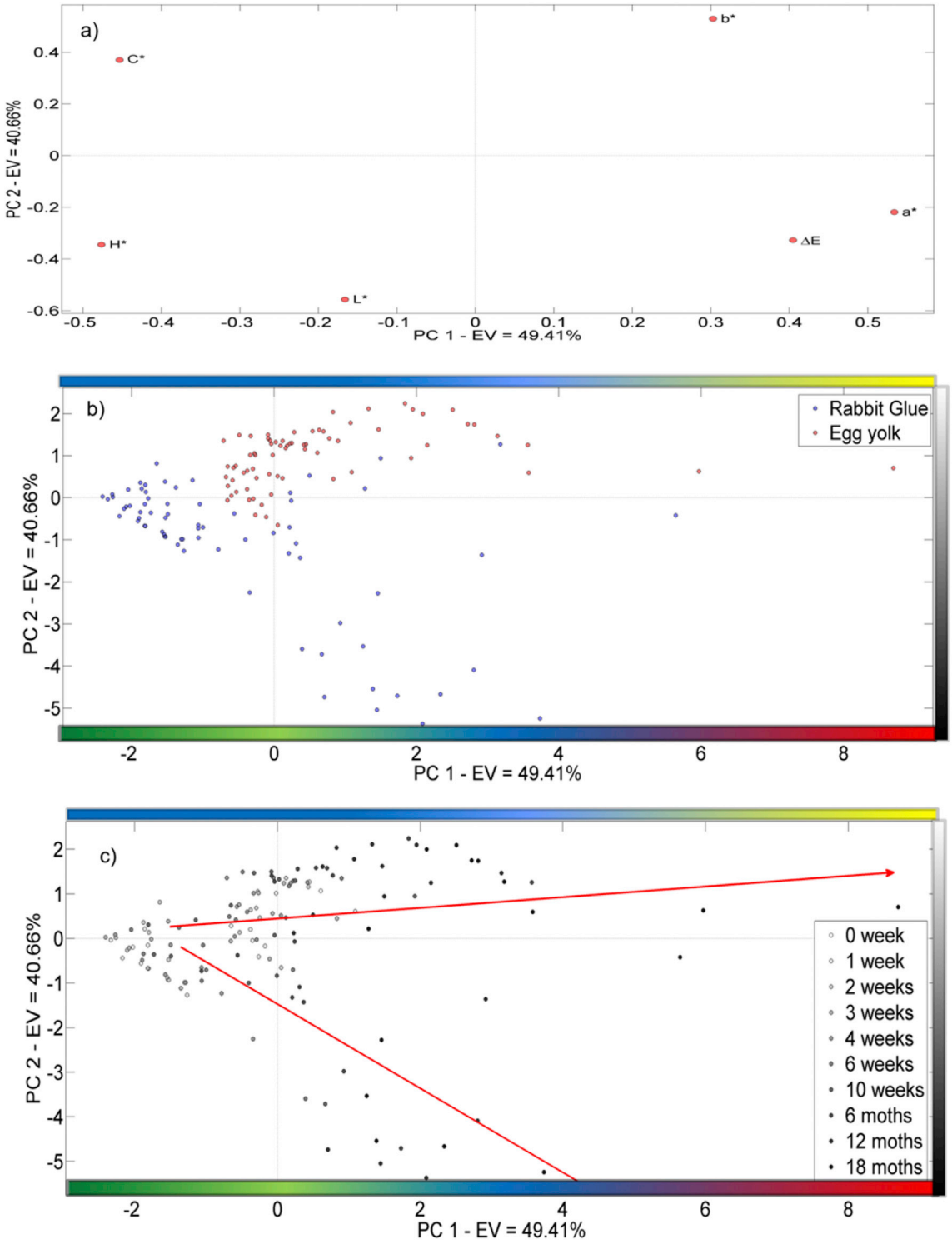

Fig. 5. PCA results for malachite-laden dosimeters: (a) loading plot PC1 *vs* PC2; (b) score plot PC1 *vs* PC2 (scores colored according to the kind of binder); (c) score plot PC1 *vs* PC2 (scores colored according to exposure times).

shows the corresponding loading (Fig. 5a) and score plots. In order to better search for some kind of pattern in the results, dosimeters are represented according to the binder (Fig. 5b) and the exposure time (Fig. 5c).

The loading plot shown in Fig. 5a revealed that the color parameters were clearly separated into four groups (easier score plot interpretation). Fig. 5b, which examines the influence of the binder in the dosimeters, shows that the type of binder was discriminated well enough in PC2, as most of the dosimeters containing egg yolk obtained scores greater than 0, while rabbit glue gave scores of less than 0. This is an interesting result as the MAL-VEF-E and MAL-VEF-G dosimeters cannot be distinguished with the naked eye. The loading plot (Fig. 5a) showed that all chromatic parameters have a high influence in PC1 with the exception of L*, which is the most influential in PC2. Consequently, luminosity appears to be the most important factor for discriminating the type of binder.

Fig. 5c shows a relationship between PC1 and exposure time, as samples are distributed according to their exposure time. In MAL-VEF-E, the tendency to yellow hues (+b*) is one of the key color parameters related to color change over time, as it presents positive loadings in both PCs, i.e. PC1 and PC2. We also noticed this in all egg yolk-based dosimeters measured at the highest exposure times. Thus, the values for MAL-VEF-E at the start of the natural aging test are characterized low b* values (blue hues), which increase in line with exposure time. This means that dosimeters containing egg yolk become yellower over time. Likewise, dosimeters containing rabbit glue binder were characterized by low b* values at the lowest measurement times. However the chromatic parameters a* (red/green) and ΔE (total color change) appear as the decisive factors affecting color variations over time, in that the greatest changes took place in these parameters. Results show that ΔE is higher for MAL-VEF-G than for MAL-VEF-E. MAL-VEF-G also turns redder with increasing exposure times.

3.2. Azurite

PCA was performed on a data matrix with 774 rows (azurite-laden samples) and 6 columns (color variables). In this multivariate analysis the first three components explained 94% of the total data variance (Table 2 supplemental file). The loading plots are shown in Fig. 6. The PC1 *vs* PC2 loading plot (Fig. 6a) once again displays that the color parameters are grouped into four types, i.e. those defined by the x/y axes. C*, H* and a* color parameters have the highest negative values on PC1, while b* has the highest positive values. The PC1 scores could therefore be related with the tendency of the paint dosimeters to turn yellower. The two remaining variables, i.e. L* and ΔE have little influence on this PC1,

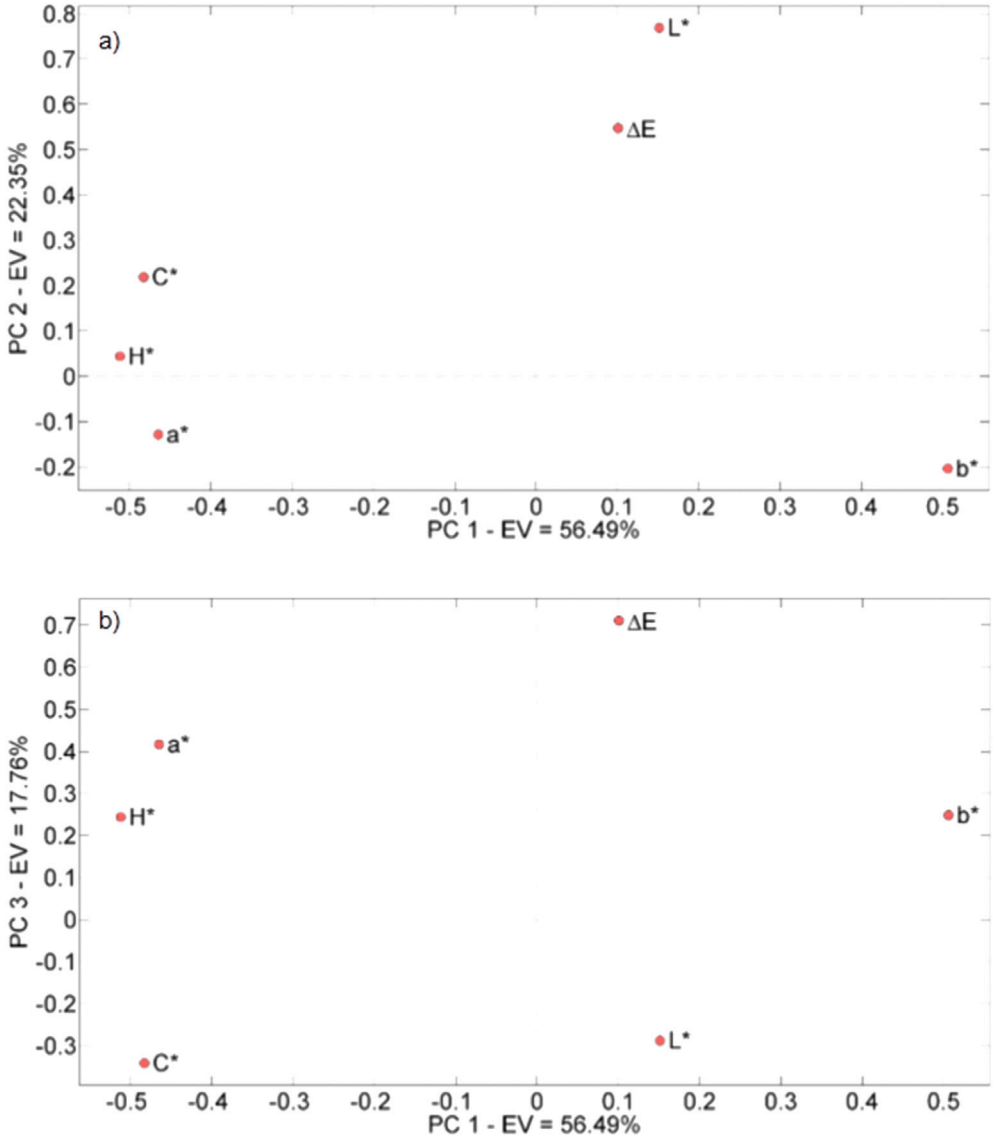

Fig. 6. Loading plots for the azurite-laden dosimeters: (a) PC1 *vs* PC2; (b) PC1 *vs* PC3.

showing higher weights on PC2. Fig. 6b shows the loading plot for PC1 and PC3. Although all the chromatic parameters show a certain dependence on PC3 with loading values far above or below zero, ΔE has the highest weight on this PC. This suggests that PC3 scores are mainly related with total color change (ΔE). Hence, dosimeters with high scores on this PC will have undergone important color modifications.

To better understand the pattern in the data, the scores were again colored according to the different parameters being investigated (Fig. 7), i.e. the kind of binder used in the paint dosimeters (Fig. 7a), exposure time (Fig. 7b) and pigment particle size (Fig. 7c and d).

Results suggested that the combination of PC1 and PC2 allowed us to distinguish the type of binder present in the dosimeters. Two clearly

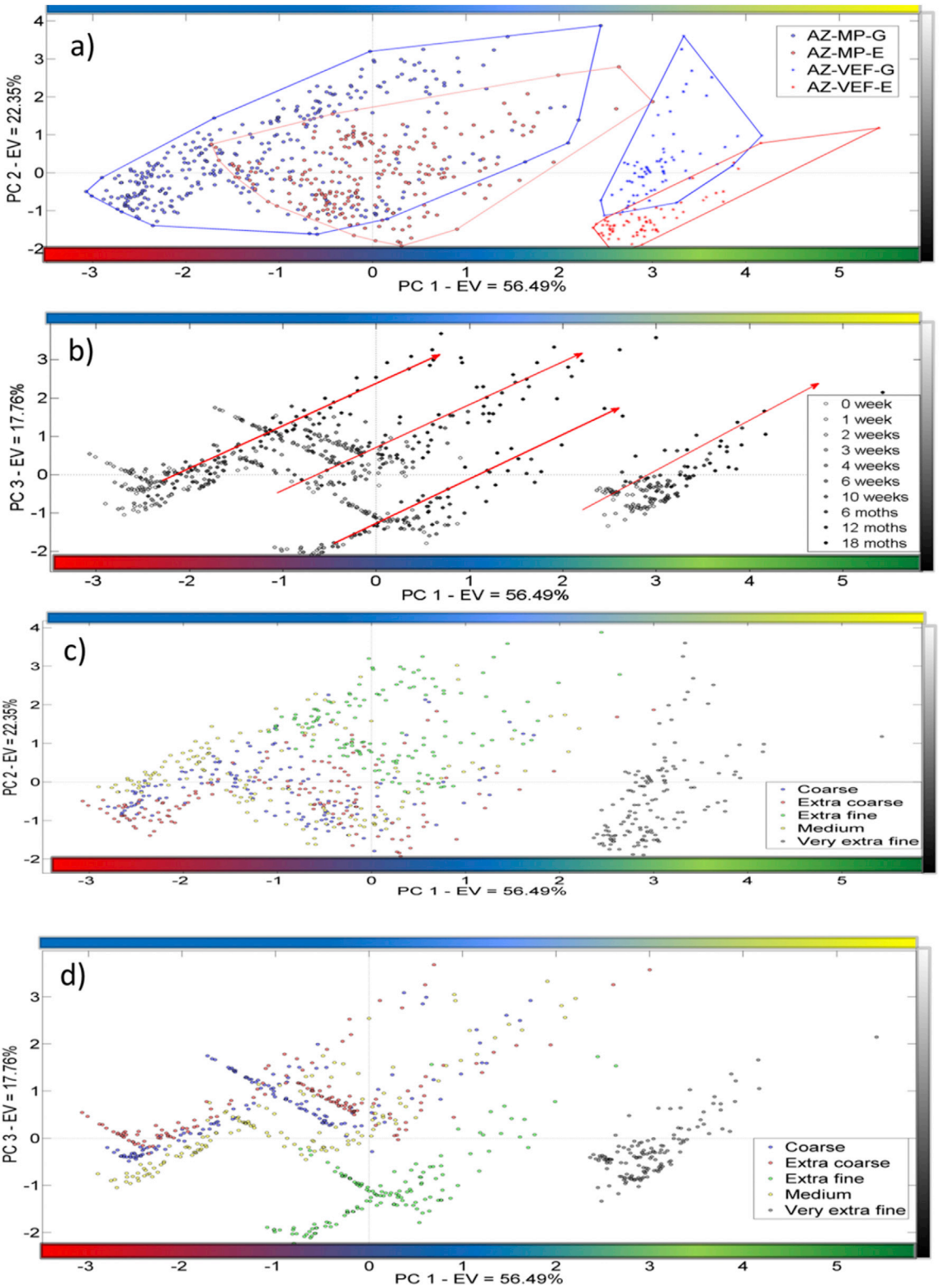

Fig. 7. Score plots for the azurite-laden dosimeters: (a) PC1 *vs* PC2 (scores colored according to the kind of binder); (b) PC1 *vs* PC3 (scores colored according to exposure times); (c) PC1 *vs* PC2 (scores colored according to grain size); (d) PC1 *vs* PC3 (scores colored according to grain size). AZ-MP means all the azurites MP (see Table 1).

differentiated groups can be observed on the score plot (Fig. 7a). One group comprises all the azurite MP samples, and the other includes the azurite standard (i.e. AZ-VEF see Table 1). This second group has two clearly distinguishable sub-groups according to the binder used in the dosimeters. At the start of the natural aging test on the dosimeters all the azurite samples were characterized by high C*, H* and +a* (red hues) values and low L* and ΔE values (i.e. ca. 4 weeks); all these parameters increased with exposure time to the urban atmosphere (Fig. 7a). This means that the azurite MP dosimeters containing rabbit glue become greener and more luminous over time.

By contrast, all the azurite MP samples mixed with egg yolk have scores closer to zero than those mixed with glue (Fig. 7a). The azurite MP dosimeters showed more disperse chromatic parameters compared to the AZ-VEF dosimeters measured over time. They also have some overlap with the other grain sizes in rabbit glue-based samples since the corresponding scores appear nearby. The azurite MP dosimeters therefore have similar H*, C* and a* (red/green) values but they have higher values of L* and ΔE with respect to the paint dosimeters with long exposure times. The AZ standard samples (i.e. AZ-VEF, see Table 1) have the highest values of +b* (yellow hues) at the shortest exposure times, in particular the AZ-VEF-E dosimeter. The score plot (Fig. 6a) and loading plot (Fig. 7a) show that as time passes the chromatic parameters L* and ΔE are the decisive factors affecting color changes over time. This means that AZ-VEF-G samples become bluer and more luminous over time, as well as experiencing the greatest net change in color, as detected by Cardell et al. [19] who noted dissolution of the glue exposing azurite crystals. For its part AZ-VEF-E was characterized by high +b* (yellow hues) values at the shortest exposure times, although over time it underwent less change in L* and ΔE than AZ-VEF-G.

The score plot for PC1 vs PC3 contains information about color changes over different exposure times (see Fig. 7b). The loading plot (Fig. 6b) showed that all the chromatic parameters had a high weight in PC1 with the exception of ΔE, which had a higher influence on PC3. ΔE appears to be the most important factor for discriminating color change due to exposure time.

Fig. 7c and d shows how PC1 separates AZ-VEF dosimeters (i.e. azurite standard according to Kremer, see Table 1) from the other MP azurites (extra coarse, coarse, medium, and extra fine grain sizes). AZ-VEF samples were characterized by high +b* (yellow hues) values, with both AZ-VEF-E and AZ-VEF-G samples having high b* positive scores and loading on PC1, respectively. Furthermore, the score plot on PC1 and PC3 (Fig. 7d) separated AZ-VEF dosimeters and AZ-EF dosimeters. AZ-VEF dosimeters became yellower (+b*) and greener (-a*) than the azurite MP dosimeters. In addition, AZ-EF dosimeters showed the highest brightness values and represent the grain size that contributed most to color change in all the azurite dosimeters.

3.3. *Lapis lazuli*

PCA was performed on a data matrix with 154 rows (lapis lazuli) and 6 columns (color variables) containing the information about all the lapis lazuli-laden dosimeters. After applying PCA, results indicated that the first two components together explained 79% of the original data variance (Table 2 supplemental file), and were thus retained for data interpretation. The corresponding loading and score plots are shown in Fig. 2 supplemental file. To better analyze the data patterns, the scores for the lapis lazuli-laden dosimeters are presented according to their binder content and the different exposure times.

Although in our initial inspection these paint dosimeters did not appear to be clustered, results suggest that there is a “hidden” relationship between the six color variables and the exposure time. The type of binder is also discriminated on PC2. The loading plot (Fig. 2 supplemental file) indicated that all the chromatic parameters had a high influence on PC1, with the exception of b* and C*, which are more important on PC2. Consequently, b* (yellow/blue) and C* (chroma) are the most important factors for discriminating the type of binder in lapis lazuli-laden dosimeters. As regards sample LAP-M-E, all the color parameters were related to the color change over time (Fig. 2c supplemental file), since the corresponding paint dosimeters had positive loadings on both PCs. This was also observed in the egg yolk-laden samples when measured at the highest exposure times. Thus, LAP-M-E dosimeters whose colors were measured at the start of the natural aging test, were characterized by low -b* (blue hues) values, which increased in line with the time exposed to the urban air. This means that paint dosimeters containing egg yolk become yellower over time. Likewise, LAP-M-G samples were characterized by low -b* (blue hues) and high +a* (red hues) values at the lowest exposure times. However in this case the chromatic parameters L* and ΔE are the decisive factors affecting color changes over time.

4. Conclusions

The information obtained by applying this innovative reliable approach based on PCA to discrete color parameters enabled us to visualize and interpret the color change trends (over time) of dosimeters exposed long-term to the urban atmosphere more easily, as well as to discriminate paint dosimeters based on their pigment/binder characteristics and composition.

The results confirmed successful discrimination of the pigment when all the dosimeters were studied together. After long periods of exposure to the polluted urban environment, lapis lazuli-laden dosimeters acquired the distinctive blue of the azurite-laden dosimeters. PCA also allowed us to discriminate between the two proteinaceous binders (egg or rabbit glue) and the different grain sizes (in the azurite-laden dosimeters). This approach thus offers an efficient, fast and non-expensive exploratory procedure to obtain important information about paint composition.

A closer, more detailed study of each of the pigment-laden dosimeters revealed sufficient differences in luminosity to discriminate the binder in azurite and malachite-laden dosimeters, in which those prepared with rabbit glue showed high luminosity values. In the case of lapis lazuli-laden dosimeters the yellowness was the discriminant parameter for the paints containing egg-yolk binder, which became yellower as exposure time increased. As a general tendency for the binder, results indicated that paint dosimeters prepared with rabbit glue tended to become brighter and those prepared with egg yolk went yellower over time. In addition, lapis lazuli and azurite-laden dosimeters tended to a slightly greener shade, especially in the presence of the egg yolk binder. By contrast, the initially green malachite-laden dosimeters turned bluer.

Results indicated that grain size was important in the greenish tendency. Thus, in the different grain sizes studied in the azurite pigments, the greenish tendency was only observed in the dosimeters with small grain azurite. The color change tendencies were similar in the dosimeters with extra coarse, coarse and medium grain sizes, as the multivariate approach could not discriminate between them.

In summary, we evaluated the natural aging of paint dosimeters when exposed to polluted urban air, offering a clear, in-depth, detailed description of the different chromatic changes that took place. The results indicate that the azurite-laden samples underwent the most important color changes over time while the malachite and lapis lazuli-laden dosimeters were the least affected. In addition to the new approach we used, all these results provide very useful, detailed information that is of great value when considering preventive strategies for the conservation of outdoor paintings.

Acknowledgements

Financial support was provided by Spanish Research Projects AER-IMPACT (CGL2012-30729) and EXPOAIR (P12-FQM-1889), the European Regional Development Fund (ERDF), the Andalusian Research Groups RNM-179 and FQM-118, and the Milano Chemometrics and QSAR Research Group. J.A. Herrera Rubia is funded by a Spanish grant

from the AERIMPACT Project (ref. BES-2013-065507). The authors thank Nigel Walkington for English revision.

Appendix A. Supplementary data

Supplementary data related to this article can be found at http://dx.doi.org/10.1016/j.chemolab.2017.05.007.

References

[1] R. Van Grieken, A. Worobiec, X-ray spectrometry for preventive conservation of cultural heritage, Pramana J. Phys. 76 (2011) 191–200.
[2] D. Camuffo, Environmental monitoring in four European museums, Atmos. Environ. 35 (2001) 127–140.
[3] S. Sánchez-Moral, L. Luque, S. Cuezva, V. Soler, D. Benavente, L. Laiz, J.M. González, C. Saiz-Jiménez, Deterioration of building materials in Roman catacombs: the influence of visitors, Sci. Total Environ. 349 (2005) 260–276.
[4] V. Kontozova-Deutsch, C. Cardell, M. Urosevic, E. Ruiz-Agudo, F. Deutsch, R. Van Grieken, Characterization of indoor and outdoor atmospheric pollutants impacting architectural monuments: the case of San Jerónimo Monastery (Granada, Spain), Environ. Earth Sci. 63 (2011) 1433–1445.
[5] N.A. Katsanos, F. De Santis, A. Cordoba, F. Roubani-Kalantzopoulou, D. Pasella, Corrosive effects from the deposition of gaseous pollutants on surfaces of cultural and artistic value inside museums, J. Hazard. Mater. 64 (1999) 21–36.
[6] B. Horemans, C. Cardell, L. Bencs, V. Kontozova-Deutsch, K. De Wael, R. Van Grieken, Evaluation of airborne particles at the Alhambra monument in Granada, Spain, Microchem. J. 99 (2011) 429–438.
[7] J. Grau-Bové, M. Strlič, Fine particulate matter in indoor cultural heritage: a literature review, Herit. Sci. 1 (2013) 1–17.
[8] M. Bacci, M. Picollo, S. Porcinai, B. Radicati, Tempera-painted dosimeters for environmental indoor monitoring: a spectroscopic and chemometric approach, Environ. Sci. Technol. 34 (2000) 2859–2865.
[9] M. Odlyha, N.S. Cohen, G.M. Foster, Dosimetry of paintings: determination of the degree of chemical change in museum exposed test paintings (smalt tempera) by thermal analysis, Thermochim. Acta 365 (2000) 35–44.
[10] R. Mazzeo, S. Prati, M. Quaranta, E. Joseph, E. Kendix, M. Galeotti, Attenuated total reflection micro FTIR characterisation of pigment–binder interaction in reconstructed paint films, Anal. Bioanal. Chem. 392 (2008) 65–76.
[11] D. Saunders, H. Chahine, J. Cupitt, Long-term colour change measurement: some results after 20 years, Natl. Gall. Tech. Bull. 17 (1996) 81–90.
[12] M. Bacci, L. Boselli, M. Picollo, B. Pretzel, Colour measurement on paintings, in: L. Tassi, M.P. Colombini (Eds.), New trends in Analytical, Environmental and Cultural Heritage Chemistry Developments, Res. Signpost, Trivandrum, 2008, pp. 333–344.
[13] E. Manzano, J. Romero-Pastor, N. Navas, L.R. Rodríguez-Simón, C. Cardell, A study of the interaction between rabbit glue binder and blue copper pigment under UV radiation: a spectroscopic and PCA approach, Vib. Spectrosc. 53 (2010) 260–268.
[14] G.D. Smith, R.J.H. Clark, The role of H_2S in pigment blackening, J. Cult. Herit. 3 (2002) 101–105.
[15] M. Cotte, J. Susini, N. Metrich, A. Moscato, C. Gratziu, A. Bertagnini, M. Pagano, Blackening of pompeian cinnabar paintings: X-ray microspectroscopy analysis, Anal. Chem. 78 (2006) 7484–7492.
[16] S. Potgieter-Vermaak, B. Horemans, W. Anaf, C. Cardell, R. Van Grieken, Degradation potential of airborne particulate matter at the Alhambra monument: a Raman spectroscopic and electron probe X-ray microanalysis study, J. Raman Spectrosc. 43 (2012) 1570–1577.
[17] A. Herrera, N. Navas, C. Cardell, An evaluation of the impact of urban air pollution on paint dosimeters by tracking changes in the lipid MALDI-TOF mass spectra profile, Talanta 155 (2016) 53–61.
[18] T. Rivas, J. Pozo-Antonio, D. Barral, J. Martínez, C. Cardell, Vectorial versus functional statistical approaches to evaluate colour variations of tempera paints exposed to real environment, in: Conf Metrol. Archaeol. Cult. Herit. (MetroArchaeo 2016), 2016.
[19] C. Cardell, A. Herrera, I. Guerra, N. Navas, L. Rodríguez Simón, K. Elert, Pigment-size effect on the physico-chemical behavior of azurite-tempera dosimeters under natural and accelerated photo aging, Dye. Pigment. 141 (2016) 53–65.
[20] L. Medeghini, S. Mignardi, C. De Vito, A.M. Conte, Evaluation of a FTIR data pretreatment method for Principal Component Analysis applied to archaeological ceramics, Microchem. J. 125 (2016) 224–229.
[21] A. Nevin, I. Osticioli, D. Anglos, A. Burnstock, S. Cather, E. Castellucci, The analysis of naturally and artificially aged protein-based paint media using Raman spectroscopy combined with Principal Component Analysis, J. Raman Spectrosc. 39 (2008) 993–1000.
[22] C. Miguel, J.A. Lopes, M. Clarke, M.J. Melo, Combining infrared spectroscopy with chemometric analysis for the characterization of proteinaceous binders in medieval paints, Chemom. Intell. Lab. Syst. 119 (2012) 32–38.
[23] K. Rajer-Kanduč, J. Zupan, N. Majcen, Separation of data on the training and test set for modelling: a case study for modelling of five colour properties of a white pigment, Chemom. Intell. Lab. Syst. 65 (2003) 221–229.
[24] S. Mas, C. Miguel, M.J. Melo, J.A. Lopes, A. de Juan, Screening and quantification of proteinaceous binders in medieval paints based on μ-Fourier transform infrared spectroscopy and multivariate curve resolution alternating least squares, Chemom. Intell. Lab. Syst. 134 (2014) 148–157.
[25] I. Osticioli, N.F.C. Mendes, S. Porcinai, A. Cagnini, E. Castellucci, Spectroscopic analysis of works of art using a single LIBS and pulsed Raman setup, Anal. Bioanal. Chem. 394 (2009) 1033–1041.
[26] E. Franceschi, P. Letardi, G. Luciano, Colour measurements on patinas and coating system for outdoor bronze monuments, J. Cult. Herit. 7 (2006) 166–170.
[27] G. Luciano, R. Leardi, P. Letardi, Principal component analysis of colour measurements of patinas and coating systems for outdoor bronze monuments, J. Cult. Herit. 10 (2009) 331–337.
[28] M. Urosevic, A. Yebra-Rodríguez, E. Sebastián-Pardo, C. Cardell, Black soiling of an architectural limestone during two-year term exposure to urban air in the city of Granada (S Spain), Sci. Total Environ. 414 (2012) 564–575.
[29] G. Titos, H. Lyamani, L. Drinovec, F.J. Olmo, G. Močnik, L. Alados-Arboledas, Evaluation of the impact of transportation changes on air quality, Atmos. Environ. 114 (2015) 19–31.
[30] C. Cardell-Fernández, C. Navarrete-Aguilera, Pigment and plasterwork analyses of Nasrid polychromed lacework stucco in the Alhambra (Granada, Spain), Stud. Conserv. 51 (2006) 161–176.
[31] C. Cardell, L. Rodríguez-Simón, I. Guerra, A. Sánchez-Navas, Analysis of Nasrid polychrome carpentry at the Hall of the Mexuar Palace, Alhambra complex (Granada, Spain), combining microscopic, chromatographic and spectroscopic methods, Archaeometry 51 (2009) 637–657.
[32] M. Price, A renaissance of color: particle separation and preparation of azurite for use in oil painting, Leonardo 33 (2000) 281–288.
[33] R. Mayer, S. Sheehan, The Artist's Handbook of Materials and Techniques, The Viking, New York, 1991.
[34] J. Schanda, Colorimetry: Understanding the CIE System, John Wiley and Sons, 2007.
[35] D. Ballabio, A MATLAB toolbox for Principal Component Analysis and unsupervised exploration of data structure, Chemom. Intell. Lab. Syst. 149 (2015) 1–9.
[36] R. Bro, A.K. Smilde, Principal component analysis, Anal. Methods 6 (2014) 2812–2831.
[37] I.T. Jolliffe, Principal Component Analysis, in: Encycl. Stat. Behav. Sci, second ed., vol. 30, 2002, p. 487.
[38] E. Sánchez-Zapata, E. Fuentes-Zaragoza, C. Navarro-Rodríguez de Vera, E. Sayas, E. Sendra, J. Fernández-López, J.A. Pérez-Alvarez, Effects of tuna pâté thickness and background on CIEL*a*b* color parameters and reflectance spectra, Food Control 22 (2011) 1226–1232.